Local structure of expanded fluid mercury using synchrotron radiation: From liquid to dense vapor

Masanori Inui*

Faculty of Integrated Arts and Sciences, Hiroshima University, Higashi-Hiroshima 739-8521, Japan

Xinguo Hong

*Beijing Synchrotron Radiation Facility (BSRF), Institute of High Energy Physics, Chinese Academy of Science,
Beijing 100039, People's Republic of China*

Kozaburo Tamura

Graduate School of Engineering, Kyoto University, Kyoto 606-8501, Japan

X-ray-diffraction measurements for fluid mercury up to the supercritical region have been carried out using synchrotron radiation at SPring-8. We obtained the structure factor $S(Q)$ with good signal-to-noise ratio, and the pair distribution functions $g(r)$ for expanded fluid Hg from the liquid to the dense vapor. To see the volume dependence of the local structure in fluid Hg in detail, we tried to reproduce $4\pi n_0 r^2 g(r)$ of fluid Hg using Gaussian peaks. The optimized parameters show that the asymmetrical first peak in $g(r)$ of liquid Hg consists of atomic distributions at short and long distances of about 3 Å and 3.5 Å. Volume dependence of the parameters suggests that decrease of the atoms coordinated at the short distance is strongly correlated with the metal-nonmetal transition in fluid Hg.

I. INTRODUCTION

Metals are finally transformed to an insulating state when they are sufficiently expanded. A simple band model predicts that divalent metals are transformed to an insulating state with volume expansion by forming an energy gap between s and p bands. Liquid Hg, well known as a prototype of divalent liquid metals, has extensively investigated so far because it undergoes the metal-nonmetal (M-NM) transition when it is expanded up to the liquid-gas critical point [critical data of Hg (Ref. 1): $T_C = 1751$ K, $p_C = 1673$ bar, $\rho_C = 5.8$ g cm^{-3}]. The first indication of the M-NM transition was found in the electrical conductivity and thermopower data obtained by Hensel and Frank.[2] Figure 1 shows the density isochores plotted in the pressure-temperature plane reported by Gözlaff.[1] A bold solid line indicates the saturated vapor-pressure curve and the closed diamond shows the critical point. Many investigations have been made focusing on the M-NM transition in fluid Hg. Measurements of electrical conductivity,[3–5] thermopower,[3,6–8] and Hall coefficient[9] indicate that, as the density is reduced, the M-NM transition starts to occur at a density of about 9 g cm^{-3}, whose isochore is denoted by a bold broken line in Fig. 1. Data of optical reflectivity[10,11] and optical absorption coefficient[12,13] support the transition around the density. The result of nuclear magnetic resonance[14] clearly indicates that the M-NM transition occurs at around 9 g cm^{-3}. Thermodynamic properties of expanded fluid mercury such as equation of states,[1,2,4,5,15,16] sound velocity,[17–20] sound attenuation,[18,21] and specific heat[22] were also investigated to clarify the mechanism of M-NM transition. Several experimental results on the transition were reviewed and discussed in the literature.[23]

Theoretical attempts were made to understand the M-NM transition in fluid Hg based on the simple band model. Devillers and Ross[24] applied a pseudopotential method to calcu-late the energy bands for crystalline Hg with expanded bcc, fcc, and rhombohedral structures. Band-structure calculations for such a uniformly expanded crystalline Hg were carried out by many others.[25,26] An alternative approach taken by Mattheiss and Warren[27] assumed that the nearest-neighbor distance was constant, so the density variation in expanded fluid Hg was due entirely to the changes in the coordination number. These theoretical studies besides Devillers and Ross show that the band gap does not appear at 9 g cm^{-3} but at much smaller density. On the other hand, an early data of the optical absorption showed that the optical gap seems to close at around 6 g cm^{-3}.[12] Bhatt and Rice[28] calculated optical absorption spectra from the gaseous state to around the critical density, on the basis of a model of excitonic absorption in clusters. They suggested that an exciton band is responsible
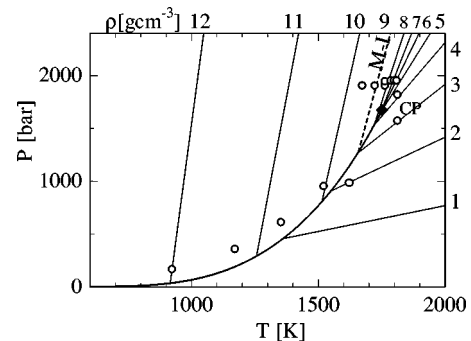

FIG. 1. The density isochores for fluid Hg plotted in the pressure-temperature plane (Ref. 1). A bold solid line indicates the saturated vapor-pressure curve and the close diamond shows the critical point. Open circles show the pressures and temperatures at which x-ray-diffraction measurements were performed. The isochore of 9 g cm^{-3} where the metal-insulator (M-I) transition occurs is denoted by a bold broken line.

for the apparent closing of the optical gap around 6 g m^{-3} and later experimental data on the M-NM transition obtained from optical absorption measurements[13] were consistent with those of electrical measurements. Since these theoretical studies could not give an exact density of the M-NM transition obtained experimentally, a possibility was pointed out that the density fluctuations near the critical point play an important role for the M-NM transition. Franz showed a model producing a gap at the correct density of 9 g cm^{-3}.[29] The model was based on the assumption of a linear decrease in the average coordination number with decreasing density, but the fact that the actual coordination number would be distributed randomly over a range around the mean number was taken into account. As another theoretical approach, Turkevich and Cohen[30] postulated the existence of an excitonic insulator phase in fluid Hg and argued that a collective effect could produce both a real gap at around 9 g cm^{-3} and another anomaly at around 3 g cm^{-3} in dense Hg vapor found by optical measurements.[31]

In this context, it is obvious that the information on the atomic arrangement of expanded fluid Hg is important for exact understanding of the M-NM transition. However, the diffraction experiments for expanded fluid Hg are quite difficult because the critical pressure is very high. For many decades we have had almost no structural studies for metallic fluids near the liquid-gas critical points, except for fluid Rb and fluid Cs. The static and dynamic structures of fluid Rb and fluid Cs were investigated using neutrons.[32] Recently, Tamura and Hosokawa measured x-ray diffraction using an in-house x-ray source for expanded liquid Hg in the metallic region and also up to the critical region at the density of 6.6 g cm^{-3}.[33–35] They obtained information about the first-neighboring coordination. The results show that the first-neighbor distance remains almost constant while the first-neighboring coordination number decreases substantially and almost linearly with decreasing density to the M-NM transition region. As correlated with the development of experimental studies, Kresse and Hafner[36] carried out an *ab initio* molecular dynamics simulation for expanded fluid Hg and obtained the density dependence of the atomic configuration consistent with the experimental data reported by Tamura and Hosokawa.[35] In particular, their simulation succeeded in showing that the gap between 6s and 6p bands appears at about 9 g cm^{-3}. Tamura and Hosokawa[35] compared their experimental results to those obtained from theoretical studies including the *ab initio* molecular dynamics simulation and speculated that an increase of fluctuations in the nearest-neighboring coordination number would strongly be correlated with the M-NM transition in fluid Hg. They also pointed out the necessity of structural information on dense Hg vapor to investigate cluster formation at lower density. As another theoretical approach, Munejiri *et al.*[37] deduced an effective pair potential as a function of density by an inverse method using experimental data[35] and carried out a large-scale molecular dynamics simulation. They studied dynamic structure of expanded fluid mercury and reported density dependence of sound velocity consistent with that which was obtained experimentally.[19]

To compare the results of recent simulations[36,37] with the experimental data, it is essential to get more information on the medium range order—such as the second- and third-neighbor coordinations—of metallic fluids and it is necessary to perform x-ray-diffraction experiments using a synchrotron radiation source instead of an in-house x-ray source. Synchrotron radiation is quite strong and directional in character. Combining our high-temperature and high-pressure techniques with synchrotron radiation we have a greater possibility to get high quality data on the microscopic structures, density fluctuations, and dynamic structure, for supercritical metallic fluids. We have made x-ray-diffraction measurements for metallic fluids up to the supercritical region using synchrotron radiation at the superphoton ring operating at 8 GeV (SPring-8) in Japan since the first operation of the facility in 1997.[38–40] Not only the quality of the data became much better than that of the previously reported ones but also the structure factor of dense Hg vapor was obtained. In this paper we report the results of x-ray-diffraction measurements for fluid Hg using synchrotron radiation at SPring-8 and discuss the change of the local structure in fluid Hg with volume expansion based on the experimental facts.

II. EXPERIMENTAL

We have performed energy-dispersive x-ray-diffraction measurements for expanded fluid metals using synchrotron radiation on the BL04B1 beam line at SPring-8. The storage ring at SPring-8 was operated at 8 GeV with 100 mA during the present experiments. White x rays irradiated from a bending magnet and collimated to 0.2×0.2 mm^2 using slits at upper stream were incident on the sample and the scattered x rays were detected with a pure Ge solid-state detector. The details of the experimental setup are described elsewhere.[40,41]

The experiments at high temperature and high pressure were performed using an internally heated high-pressure vessel made of a super-high-tension steel. The apparatus permits measurements to be made up to 2000 K and 2000 bar. The high-pressure vessel for x-ray-diffraction measurements has seven Be windows for the scattered x-ray beams, which are located at the scattering angles of 2θ of 4, 7, 11.5, 15, 20, 25, and 33°, to cover a sufficiently wide range of scattering wave number Q ($Q = 4\pi E \sin\theta/hc$, where h is Planck's constant, c is the velocity of light, and E is the energy of the x ray). The construction of the high-pressure vessels is shown elsewhere.[41] The vessel is pressurized by He gas of high-purity grade (99.9999%).

Supercritical fluid Hg must be contained in a cell made of a special material being transparent to x rays and resistant to chemical corrosion by hot metallic fluids. A single-crystalline sapphire cell was developed for this purpose and the details are described elsewhere.[42] The cell consists of a hot part and a sample reservoir kept around the melting temperature of the liquid sample. The hot part was heated by a *W* heater surrounding a Mo tube of 6 mm in outer diameter and 4 mm in inner diameter to keep the temperature uniform. The sapphire cell of 4 mm in outer diameter was put into the Mo tube. The temperature of the sample was measured by two Pt-30%Rh:Pt-6%Rh thermocouples, which were inserted in

the holes of the Mo tube and were in close contact with the wall of the sapphire cell. Cells with sample thicknesses of 110 μm and 260 μm were prepared and the Hg sample of high-purity grade (99.999%) was used for the present experiments.

The observed data were analyzed principally using the same procedure reported in the previous paper[35] and it is briefly summarized as follows. We measured x-ray-diffraction spectra of an empty cell, and those of fluid Hg after liquid Hg was, *in situ*, loaded into the cell and a uniform liquid thin film was formed at the hot part. First, tiny distortion of the spectra by escape effect of the Ge solid-state detector was corrected. Second, to estimate the energy spectrum of the primary beam $I_0(E)$, the spectrum of the empty sapphire cell was analyzed on the assumption that it consists of Compton scattering from Al and O atoms. The assumption was almost satisfied because the crystalline axes of the cell were adjusted and strong Laue spots from the cell were not directed to the detector at the scattering angles. To deduce $I_0(E)$, corrections for the absorption by the cell and Be windows of the high-pressure vessel were made. The profiles of $I_0(E)$ obtained were similar to synchrotron radiation spectrum calculated theoretically for a bending magnet at SPring-8 if the efficiency of the solid-state detector and absorption by the air are taken into account. Then the spectra of fluid Hg at each temperature and pressure were analyzed. To deduce $S(Q)$, absorption by fluid Hg and compressed He gas in addition to that by the cell and Be windows, and Compton scattering from Hg were taken into account. After subtracting terms by the empty cell and Compton scattering by Hg atoms from the spectrum, a remaining coherent term was normalized by a scattering intensity estimated for an isolated Hg atom. Effects by multiple scattering were ignored at the present analysis. Numerical data such as densities,[1] mass absorption coefficients,[43] and atomic form factors for coherent[44] and incoherent[45] scatterings were cited from literatures. Finally, $S(Q)$ obtained at scattering angles were overlapped and averaged in a suitable Q range. As $S(Q)$ in larger Q region had to oscillate around $S(Q)=1$, ambiguity for selecting a suitable Q range and averaging them was very small and $S(Q)$ data obtained at different angle settings for fluid Hg have an excellent consistency in the same Q region as that shown in the previous paper.[46] However, $S(Q)$ from the first peak to the first minimum has rather large ambiguity because available Q region at small scattering angles was narrow and a small error in the process of overlap at large Q would be most amplified here. In our experience, the height of the first peak may have an inevitable error within 10% and it is a weak point of energy-dispersive method that should be overcome in future. At present we checked the $S(Q)$ curve around the first peak by performing Fourier transform and back-transform as described in the following paragraph.

The pair distribution function $g(r)$ is obtained by a normal Fourier transformation using Eq. (1):

$$g(r)=1+\frac{1}{8\pi^3 n_0}\int_0^\infty Q(S(Q)-1)\frac{\sin Qr}{Qr}4\pi QdQ. \quad (1)$$

The transformation requires the $S(Q)$ data from $Q=0$ to ∞. A lack of exact data at small Q values is not so serious from a metallic liquid to the M-NM transition region because $S(0)$ values are not so large and the $Q(S(Q)-1)$ function is very small in this region. However, in the region from the fluid near the critical density to dense Hg vapor, $S(0)$ becomes very large and the ambiguity of $S(Q)$ from $Q=0$ to Q_{min} of about 1 $\text{\AA}^{-1}$ may cause serious errors in $g(r)$. As the most reliable way, as long as we could at the present, the $S(0)$'s were calculated using the experimentally obtained isothermal compressibility of expanded fluid Hg (Refs. 1 and 4) and the interpolation of $S(Q)$ from $Q=0$ to Q_{min} was carried out using the scattering law of the Ornstein-Zernike equation with the correlation length estimated from small angle x-ray-scattering measurements.[47] In addition, the termination of the data at $Q_{max}<\infty$ introduces distinct error in the resultant $g(r)$, which mainly appears as unphysical ripples in $g(r)$ function. Tamura and Hosokawa[35] made the termination correction using a method proposed by Kaplow *et al.*[48] They repeated Fourier transform and Fourier back-transform till a reasonable $g(r)$ function was obtained. The $g(r)$ reported by them has few ripples around the main peaks. On the other hand, we performed Fourier back-transformation to see the error in the first peak region of $S(Q)$. When $S(Q)$ was obtained from an incorrect normalization, the $g(r)$ function deduced had spurious peaks in $r<d_a$, where d_a corresponds to atomic diameter of Hg. To obtain $g(r)$ free from spurious peaks we found that $S(Q)$ around the first peak and the first minimum had to be modified while $S(Q)$ in larger Q values is unchanged. The first peak region in $S(Q)$ could have a large error as already mentioned. So we renormalized the experimental data till a profile of $g(r)$ became reasonable. It should be noted that this is not a unique mathematical procedure but a semiempirical one with a physical meaning, as pointed out by Kaplow *et al.*[48] We did not perform the termination correction because quality of our $S(Q)$ data is much better than that measured using in-house x-ray source[35] and the present $g(r)$'s agree well with those reported at similar densities.

In the previous paper,[46] we estimated the densities of fluid Hg from the measured temperature and pressure points on the phase diagram.[1] However, especially in the region near the critical density, a small difference between the temperature of the sample at the position irradiated with x ray and that of the position of the thermocouples would give a large deviation between the estimated density and the real one. We corrected the real density of the sample by the following method. The absorption coefficient of the sample becomes large with increasing density and this fact means that the onset of the observed x-ray-diffraction spectrum is shifted to higher energy with increasing density. The densities estimated from the shift were in good agreement with those obtained from the phase diagram at the measured temperature and pressure except for the density region from 5 to 8 g cm^{-3}. For the sample thickness of 110 μm, the densities of 7 and 8 g cm^{-3} evaluated from the measured temperature and pressure were corrected to be 5.8 and 7.6 g cm^{-3}, respectively, while for the thickness of 260 μm, 5.8, 6.6, 7.4, and 8.4 g cm^{-3} were corrected to 5.0, 5.3, 5.7, and
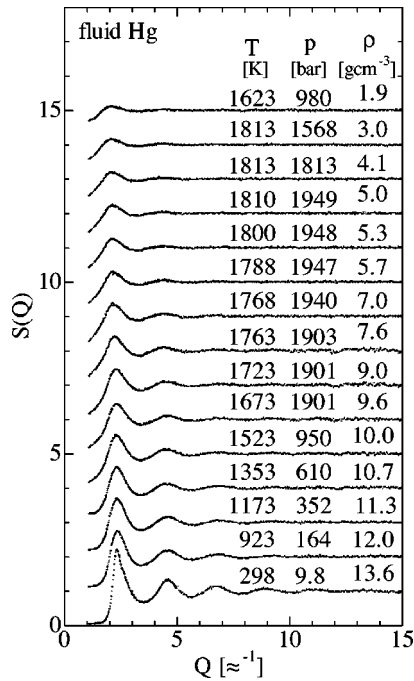
FIG. 2. Structure factor $S(Q)$ for expanded fluid Hg. Temperature, pressure, and density are indicated at the upper right-hand side of each of the data points. The curves have been displaced for clarity.

7.0 $\mathrm{g\,cm^{-3}}$, respectively. These corrections of density correspond to a correction of temperature within 20°. Note that we show temperatures measured by the thermocouples without correction in Figs. 2 and 3. We did not correct pressure because it was measured using Heise gauge with the accu-
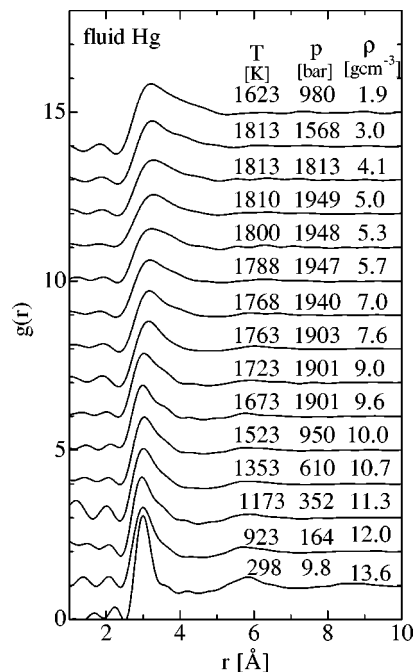
racy of ±5 bar at 2000 bar and, in principle, the same pressure was transmitted to the sample.

III. RESULTS

We have carried out x-ray-diffraction measurements for expanded fluid Hg in the temperature and pressure ranges to 1813 K and 1949 bar along the saturated vapor-pressure curve and with densities ranging from 13.6 to 1.9 $\mathrm{g\,cm^{-3}}$. The measured points are indicated in Fig. 1 by open circles. Figure 2 shows the $S(Q)$ for expanded fluid Hg in different temperatures and pressures. Dots denote the experimental data and they seem to draw a continuous curve. Note that in the previous data reported[35] dots of the same definition scatter but their smoothed curve is in good agreement with our dots at similar density.

Figure 3 shows the pair distribution function $g(r)$ calculated from the Fourier transforms of $S(Q)$, of fluid Hg shown in Fig. 2. The data for $g(r)$ at 298 K and 9.8 bar have several features; the first peak has an asymmetric shape, the first minimum is invariant in the region from 4 to 5 Å, and the second peak is rather small. The data for $g(r)$ at 298 K and 9.8 bar are in agreement with the previous data at normal condition.[49] With increasing temperature and pressure, with decreasing density, the long-range oscillation of $g(r)$ diminishes. The broadening of the first peak gradually occurs but no change of the peak position is observed and the asymmetry of the first peak remains even at temperatures and pressures up to 1768 K and 1940 bar. While the first peak is observable even in the M-NM transition region, the second peak around 6 Å is substantially damped. It should be noted that the shape and the position of first peak change when the density further decreases and the dense vapor region is approached.

IV. DISCUSSION

To obtain the definite coordination number N from the diffusive and broad $g(r)$ pattern of the liquid we employed two different methods to define and to integrate the first-neighbor peak as shown in the inset of Fig. 4. The first one (method A) is the method of integrating $4\pi r^2 n_0 g(r)$ from d_a up to the maximum position of $g(r)$, r_1, and taking twice the integral, where n_0 denotes the average number density of Hg. The second one (method B) is the method of integrating $4\pi r^2 n_0 g(r)$ up to the first minimum position of $g(r)$, r_{min}. We fixed r_{min} as 4.5 Å in the whole density range because r_{min} does not change so much except in the dense vapor region.

The coordination numbers N_A and N_B obtained by the methods A and B, respectively, are plotted in Fig. 4 as a function of density. The nearest-neighbor distance r_1 is also shown at the bottom of Fig. 4. N_B decreases substantially and linearly with decreasing density in the wide region from liquid to dense vapor. On the other hand, N_A also decreases almost linearly with decreasing density in the metallic region but when the M-NM transition region is approached, i.e., around 9–10 $\mathrm{g\,cm^{-3}}$, the deviation from the linear dependence comes out. It should be noted that the density around

FIG. 3. Pair distribution function $g(r)$ for expanded fluid Hg obtained from Fourier transform of $S(Q)$ shown in Fig. 2. The curves have been displaced for clarity.
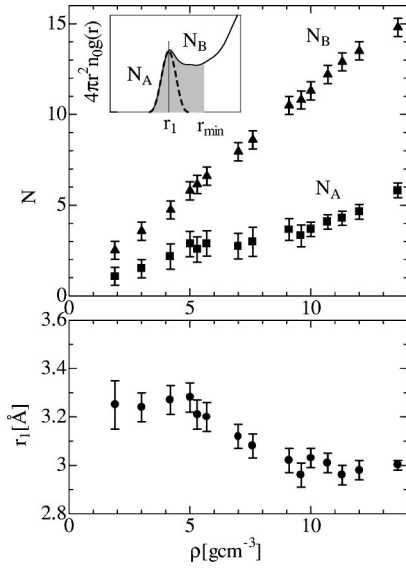
FIG. 4. The coordination number N_A, N_B denoted by closed squares and triangles, respectively, and the nearest-neighbor distance r_1, denoted by closed circles, for expanded fluid Hg as a function of density. The definition of N_A and N_B is shown in the inset and described in the text.

FIG. 5. The optimized coordination numbers N_S and N_L, peak positions, r_S and r_L, and the mean-square displacements σ_S and σ_L for the first (S) and second (L) shells, respectively, as a function of density. These two peaks mainly contribute to reproducing the asymmetrical first peak in $g(r)$.

which the deviation starts to occur coincides with the region where the M-NM transition starts to occur. On the contrary, no anomalous behavior is observed in that of N_B around this density region. In the region near the critical density, variation of N_A changes again. As seen in the figure, r_1 in the metallic region remains almost unchanged with decreasing density but when the M-NM transition region is approached, r_1 starts to slightly increase. Such a behavior coincides with the deviation from linear dependence of N_A. In the region near the critical density, r_1 becomes about 3.3 Å. The value of r_1 seems close to the interatomic distance of a Hg dimer in the rarefied vapor.[50] From these results we can conclude that the density decrease of fluid Hg is essentially caused by the reduction of the coordination number through the whole density region as seen in the behavior of N_B. The volume expansion of liquid Hg in the metallic region is not a uniform expansion with a fixed coordination number, but is caused by a decrease of coordination number with a fixed nearest-neighbor distance as concluded by Tamura and Hosokawa.[35]

To see the volume dependence of the local structure in fluid Hg in detail, we tried to reproduce $4\pi r^2 n_0 g(r)$ of fluid Hg from the liquid to dense Hg vapor using a summation of Gaussian peaks shown in Eq. (2):

$$4\pi r^2 n_0 g(r) = \sum_i \frac{N_i}{\sqrt{2\pi}\sigma_i} \exp\left(-\frac{(r-r_i)^2}{2\sigma_i^2}\right). \qquad (2)$$

Here N_i, r_i, and σ_i denote the coordination number, the interatomic distance, and the mean-square displacement of r_i for the ith shell, respectively. The least-square fitting was carried out for $4\pi r^2 n_0 g(r)$ from d_a to around 6 Å. The optimized parameters of the first and second shells are plotted as a function of density in Fig. 5. Hereafter these shells
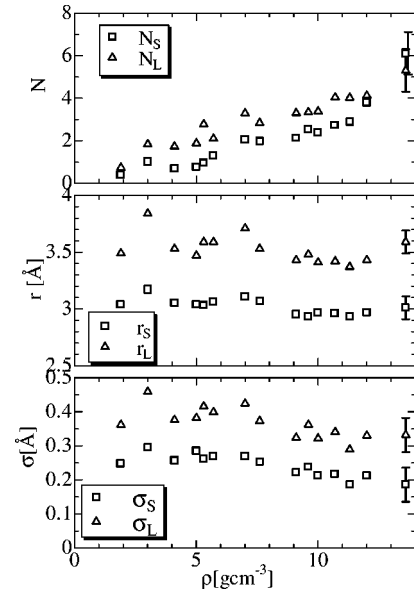
expressing the asymmetrical first peak are denoted by S and L instead of 1 and 2, respectively.

First we discuss structural change with volume expansion from liquid at normal condition to fluids near the M-NM transition. Since an x-ray-diffraction measurement for liquid Hg by Kaplow *et al.*,[48] the local structure of liquid Hg is pointed out to be similar to that of crystalline α-Hg with rhombohedral form. Figure 6(a) shows a schematic illustration of the crystal structure of α-Hg.[51] The crystal has an atomic configuration of distorted fcc structure, where six neighboring atoms are hexagonally arranged at 3.5 Å around a central atom and other six atoms are located at 3.0 Å in
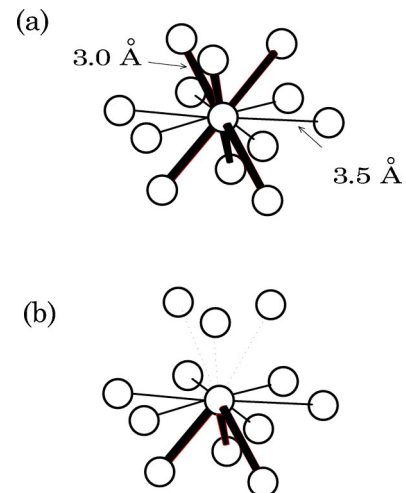

FIG. 6. (a) A schematic illustration of crystalline Hg with rhombohedral form (α-Hg). (b) An image of local structure at the first stage of volume expansion.
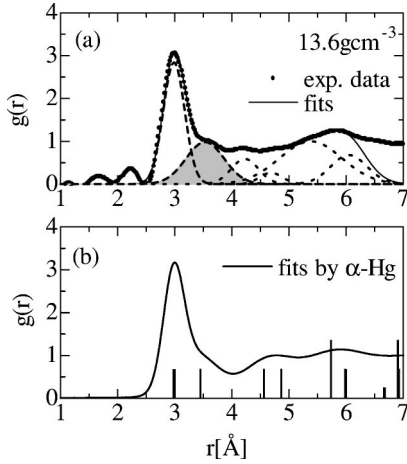
FIG. 7. (a) $g(r)$ at 13.6 g cm^{-3} reproduced using a Gaussian model. The least-square optimization was carried out for the $4\pi r^2 n_0 g(r)$ from d_a to about 7 Å. The optimized parameters of the first and second shells are shown in Fig. 5. (b) $g(r)$ reproduced using a Gaussian model in accordance with the local structure of α-Hg. The position of bars in the figure displays the interatomic distances in local structure of α-Hg and the height of bars is proportional to the number of atoms.

upper and lower planes three by three. Figure 7(a) shows the Gaussian fitting for $g(r)$ at 13.6 g cm^{-3} and the asymmetrical first peak of $g(r)$ for liquid Hg is well reproduced using two Gaussian peaks, whose positions are 3.0 Å and 3.6 Å, respectively. Their coordination numbers are about 6 and 5, respectively.

Then we confirmed if the local structure of α-Hg could reproduce the experimental $g(r)$ at 13.6 g cm^{-3}. Figure 7(b) shows the best fits using the interatomic distances $r_{\alpha i}$ and coordination numbers $N_{\alpha i}$ of α-Hg. Here we optimized the data using Eq. (2) and chose a scaling factor C_n of the coordination number, and that of the distance C_r the widths of Gaussian peaks of σ_S and σ_L, and a scaling factor of the width C_w as free parameters (that is, $r_i = C_r \times r_{\alpha i}$, $N_i = C_n N_{\alpha i}$ for $i \geq 1$, and $\sigma_i = C_w r_i$ for $i \geq 3$). The optimized values of C_n, C_r, σ_S, σ_L, and C_w were 0.917, 1.00, 0.178, 0.364, and 0.0875, respectively. The asymmetry of the first peak is well reproduced and the correlation around 6 Å appears with the crystalline parameters but there appears a hump around 4.7 Å that is not observed in $g(r)$ of the liquid. That means a limitation of this model for liquid Hg without long-range order. With decreasing density, the height of the first peak in $g(r)$ decreases. Figure 8 shows the results of Gaussian fitting for fluids at 12.0 and 9.0 g cm^{-3} together with 4.1 g cm^{-3}. The peak positions of r_S and r_L are slightly shifted to smaller distance. N_S substantially decreases while decrease of N_L is smaller. These results suggest that at the first stage of volume expansion, Hg atoms are not randomly taken away one by one from the atomic positions but especially from closer neighbors. The process is schematically illustrated in Fig. 6(b). In the liquid with large disorder, a clear cluster shown in Fig. 6(b) cannot exist. However an image, which shows that volume expansion between layers is preferred at least at the first stage of the expansion process, may help in the understanding of the present experimental
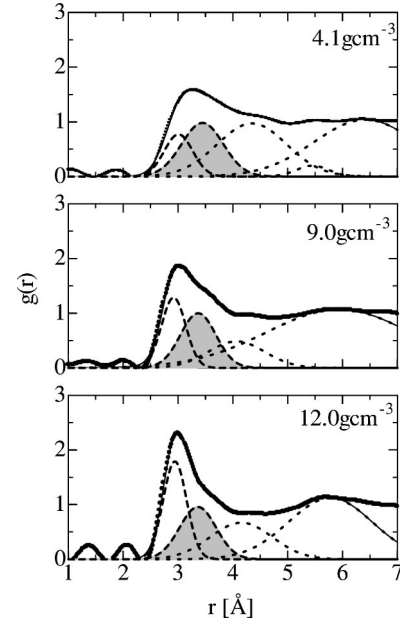

FIG. 8. $g(r)$ at 12.0, 9.0, and 4.1 g cm^{-3} reproduced using a Gaussian model. The least-square optimization was carried out for the $4\pi r^2 n_0 g(r)$ from d_a to about 6 Å. The optimized parameters of the first and second shells are shown in Fig. 5.

results. These results suggest that the decrease of atoms coordinated at 3.0 Å is closely correlated with the M-NM transition in fluid Hg. The result may also show that the average distance of the first and second coordination shells at 3.0 Å and 3.5 Å increases with decreasing density to the M-NM transition region though r_1 is constant.

In the previous paper,[41] the density variation of N_A, which represents the atomic configuration at the shortest distance in the asymmetrical first peak, was discussed, and a possibility was suggested that it is strongly related to the M-NM transition. Reverse Monte Carlo modeling technique to the x-ray-diffraction data of expanded fluid Hg using an in-house x-ray source[35] was applied by Nield and Verronen[52] and Arai and McGreevy.[53] Their analyses pointed out that the variation of the near neighbors at shorter and longer distances in the first coordination shell is important to understand the nature of the M-NM transition. The suggestion by these studies is consistent with the results of the present Gaussian fitting.

Next we discuss a local structure in dense Hg vapor from 5.7 to 1.9 g cm^{-3}. $S(Q)$ at 5.7 g cm^{-3} has clear first and second peaks, and the peaks become broad with decreasing density. As a characteristic feature, the $g(r)$ of dense Hg vapor has rather broad first peak around 3.3 Å, with a tail extending to 4–5 Å where the first minimum of liquid Hg exists. The results of Gaussian fitting show that r_S and r_L values remain the same near the metallic region while N_S and N_L decrease and become about 1 and 2, respectively. The tail around 4–5 Å in $g(r)$ comes from the third shell as shown in Fig. 8. To understand the atomic distribution around 4–5 Å, information on Hg vapor may be helpful. Barocchi et $al.$[54] measured depolarized interaction-induced light scattering spectra of Hg vapor and investigated both the form of the interaction-induced pair polarizability anisotropy

and pair potential of Hg atoms. Their results show that gaseous Hg behaves quite differently from noble gases and Hg pair develops a large intermediate-range positive anisotropy during collision. The excess polarizability anisotropy calculated based on the classical dipole-induced-dipole approximation becomes large around 3–4 Å.[23] They also estimated $g(r)$ from a model potential.[54] The distance of 4–5 Å is close to the maximum position of $g(r)$ calculated for Hg vapor at 1073 K. According to these facts, the present results may suggest that there exists a rarefied region in dense Hg vapor due to large density fluctuations and that the local structure observed by x-ray diffraction is an average of that in dense and rarefied regions. On the other hand, another explanation may be possible. The optimized N_3 of dense Hg vapor scattered at the present analysis and N_3 was located within 4 ± 2. If every third neighbor is bridged by the first neighbors of three ($= N_S + N_L$), N_3 is estimated to be 6. This estimation and optimized N_3 may support the assumption that atoms in the third shell are always bridged by another atom in the first neighbors around 3–3.5 Å. When the assumption is accepted, a bond angle of about 90° is estimated from these distances. The increase of probability that atoms are distributed around 4–5 Å with decreasing density may suggest that a bond angle of about 90° become preferable with volume expansion. It is, however, difficult to conclude which picture is proper at the present stage. To understand exact local structure, information on the density fluctuations in the supercritical fluid is of great importance.

It is a theme of interest to study what happens in the density region from 8 to 6 g cm^{-3}. Semiconducting properties of the fluid are known to be enhanced in this region. The optical gap appears in the process while Bhatt and Rice[28] proposed existence of an excitonic absorption band around 6 g cm^{-3}. Experimentally it is difficult to measure structural data in this region under stable conditions because the isochores are concentrated to the critical point and a small fluctuation of temperature can cause variation of the state of the fluid. Fluctuations near the critical point may play the most important role in this region. The present results of N_i, r_i, and σ_i ($i = S, L$) are located between the M-NM transition region and dense vapor region while data points are not many. The first peak of $g(r)$ becomes broad and approaches to the profile of dense Hg vapor. These facts suggest that the local structure of the fluid varies in this region with volume expansion as well as the electronic state.

Tamura and Hosokawa[35] discussed structural change in the M-NM transition from the microscopic point of view. They pointed out that a linear decrease of the coordination number changes around 12 g cm^{-3} in the metallic region and it may correspond to the transition from a weak scattering regime to a strong scattering one proposed by Cohen and Jortner[55] and later El-Hanany and Warren.[14] The present data have points in the metallic region less than those by Tamura and Hosokawa and it may be difficult to conclude it based on the density dependence of the coordination number. However, the quality of the present data is much better and the results of Gaussian fitting may solve their speculation. As shown in Fig. 5, a crossover between N_S and N_L occurs around 12 g cm^{-3}. Because an electron would easily transfer

to close neighboring site, it is plausible that the decrease of N_S in the metallic region affects the mechanism of the electronic transport in the fluid.

The results by Tamura and Hosokawa[35] shows that the nearest-neighbor distance starts to elongate around 9–10 g cm^{-3}. Our data agree with their results and clearly show that the elongation continues up to the critical density. As already mentioned, several band-structure calculations were carried out for the hypothetical forms of crystalline Hg. One of the approaches whose principle was consistent with the present experimental results was that of Mattheiss and Warren.[27] They assumed that the nearest-neighbor distance was constant, so the density variation in expanded fluid Hg was due entirely to the changes in the coordination number for crystalline Hg with fcc, bcc, sc, and diamond structures. They found that the trend of the density dependence of the theoretically calculated density of states (DOS) is in good agreement with that of the Knight shift in the density range down to about 9.5 g cm^{-3}. However, their hypothetical crystal with diamond structure with $N_1 = 4$, which corresponds to $\rho = 5.4$ g cm^{-3} by the interpretation of Warren and Hensel[56] using revised density data, indicates a semimetallic DOS, and it was found necessary to increase the lattice constant by 1% to fully open a gap. The experimental data of the nearest-neighbor distance show that elongation of 1% would be possible near 9 g cm^{-3} with volume expansion.

By taking fluctuations in the local coordination number into account, Franz[29] showed that a gap opens at the correct density of 9 g cm^{-3}. The model was based on the assumption that the average coordination number decreases linearly with decreasing density but that the actual local coordination numbers would randomly be distributed over a range allowed physically. The previous calculation[27] showed that for $N_1 = 4$ a gap is just before the opening while for $N_1 = 3$ a gap should exist. Franz postulated that the local gap at the atom with coordination number smaller than 4 plays a role as if a vacancy in hopping of conduction electrons and that a real gap appears when such vacancies against the transport propagate throughout the liquid. Tamura and Hosokawa[35] discussed the reliability of the model comparing the coordination numbers predicted by the model with their experimental results. They concluded that the mean coordination number of 6.7 at the M-NM transition predicted by the model would be overestimated compared to their result of 5.8. Exact definition of the coordination number in the fluid with large disorder is quite difficult. But our Gaussian fitting procedure may take account of contribution of the tails from higher shells. The coordination number in the first peak region ($= N_S + N_L$) is about 5.5, which is close to 5.8 reported in the previous work.[35] The present results suggest that when N_S becomes less than 3, the M-NM transition starts to occur. This coordination number may be consistent with the number predicted by the theoretical study.[29]

Kresse and Hafner[36] made a theoretical investigation on the density variation of the structural and electronic properties of expanded fluid Hg using an *ab initio* density-functional molecular dynamics method. They found that a single-particle gap between the 6s and 6p bands opens at a density of about 8.8 g cm^{-3}. They could well reproduce the

volume expansion in fluid Hg, which does not result in an increase of the mean interatomic distance r_1, but result in a decrease of the average coordination number. In addition, the asymmetry of the first peak in $g(r)$ was reproduced in their calculated results over the whole density range. But, as Tamura and Hosokawa[35] pointed out, r_1 in the simulation remains constant to 5.8 g cm^{-3} while our experimental results show that a clear increase of r_1 starts around 9–10 g cm^{-3} with volume expansion. They also pointed out that increase of the fluctuations in the nearest-neighboring coordination number plays the most important role in the M-NM transition around 9 g cm^{-3}. Although it is impossible to see fluctuations in the coordination number through the present analysis, the fluctuations may be correlated with the distribution of interatomic distances. The present results show that σ_S and σ_L become large from 13.6 to 7 g cm^{-3} with volume expansion as seen in Fig. 5. This evidence may support their speculation.

Finally, in $g(r)$ at 13.6 g cm^{-3} the second peak is observable around 6 Å. With volume expansion, the first peak remains but the second peak is substantially damped in the M-NM transition region. Tamura and Hosokawa[35] discussed this fact and speculated a possibility of forming small clusters such as Hg dimers ($N_1=1$), triangles ($N_1=2$), or tetrahedrons ($N_1=3$) near the critical region. Coexistence of "van der Waals–type" dimercury Hg$_2$ with the M-NM transition density was intuitively predicted by Hensel.[23] In the present results, r_1 of dense Hg vapor seems to be close to the bond distance of a Hg dimer and we speculate a possibility of forming a Hg dimer in dense vapor from the profile of $g(r)$. However, no direct evidence was obtained for such a cluster at present. To obtain the information on the cluster formation in fluid Hg experimentally, it is essential to know the exact information on fluctuations and to study dynamic properties such as inelastic-scattering measurements. We have already started to carry out small angle x-ray-scattering and inelastic x-ray-scattering measurements for expanded fluid Hg using synchrotron radiation at SPring-8 and the existence of such aggregates may be manifested in near future. Studies of advanced computer simulation will provide useful information on this subject.

V. CONCLUSION

We have carried out x-ray-diffraction measurements for supercritical fluid Hg using a synchrotron radiation source at SPring-8 since the first operation of the facility. Our experimental data are in good agreement with those reported by Tamura and Hosokawa[35] and their conclusion was confirmed. In addition, $S(Q)$ of dense Hg vapor was obtained and the variation of the local structure of fluid Hg from liquid to dense vapor shows that at least three different regions in the density exist. The first one is the metallic region from 13.6 g cm^{-3} to the M-NM transition region, where r_1 is constant and the coordination number at smaller distance of 3.0 Å decreases substantially. The present experimental evidence strongly suggests that Hg atoms are not randomly taken away one by one from the random array with a constant nearest-neighbor distance but at the first stage of the expansion, atoms at shorter distance are selectively taken away. The second one is the region from around 9 g cm^{-3} to the critical density, and the third one is the dense vapor region. It would be necessary to understand the local structure in the latter two regions, taking the effects of the density fluctuations into account.

---

*Electronic address: inui@mls.ias.hiroshima-u.ac.jp; URL: http://home.hiroshima-u.ac.jp/masinui/

[1] W. Gözlaff, G. Schönherr, and F. Hensel, Z. Phys. Chem., Neue Folge **156**, 219 (1988); W. Gözlaff, Ph.D. Thesis, University of Marburg, 1988.

[2] F. Hensel and E.U. Franck, Ber. Bunsenges. Phys. Chem. **70**, 1154 (1966).

[3] R.W. Schmutzler and F. Hensel, Ber. Bunsenges. Phys. Chem. **76**, 53 (1972).

[4] G. Schönherr, R.W. Schmutzler, and F. Hensel, Philos. Mag. B **40**, 411 (1979).

[5] M. Yao and H. Endo, J. Phys. Soc. Jpn. **51**, 966 (1982).

[6] L.J. Duckers and R.G. Ross, Phys. Lett. A **38**, 291 (1972).

[7] F.E. Neale and N.E. Cusack, J. Phys. F: Met. Phys. **9**, 85 (1979).

[8] M. Yao and H. Endo, J. Phys. Soc. Jpn. **51**, 1504 (1982).

[9] U. Even and J. Jortner, Philos. Mag. **25**, 715 (1972); Phys. Rev. B

8, 2536 (1973).

[10] H. Ikezi, K. Schwarzenegger, A.L. Simons, A.L. Passner, and S.L. McCall, Phys. Rev. B **18**, 2494 (1978).

[11] W. Hefner, R.W. Schmutzler, and F. Hensel, J. Phys. (Paris) **41**, C8-62 (1980).

[12] H. Uchtmann and F. Hensel, Phys. Lett. **53A**, 239 (1975); H. Uchtmann, U. Brusius, M. Yao, and F. Hensel, Z. Phys. Chem., Neue Folge **156**, 151 (1988).

[13] M. Yao, K. Takehana, and H. Endo, J. Non-Cryst. Solids **156-158**, 807 (1993).

[14] U. El-Hanany and W.W. Warren, Jr., Phys. Rev. Lett. **34**, 1276 (1975).

[15] M. Ross and F. Hensel, J. Phys.: Condens. Matter **8**, 1909 (1996).

[16] S. Nagel, R. Redmer, and G. Röpke, J. Non-Cryst. Solids **205-207**, 247 (1996).

[17] Suzuki, M. Inutake, S. Fujiwara, M. Yao, and H. Endo, J. Phys.

(Paris) **41**, C8-66 (1980).

[18] V. Kozhevnikov, D. Arnold, E. Grodzinskii, and S. Naurzakov, J. Non-Cryst. Solids **205-207**, 256 (1996).

[19] M. Yao, K. Okada, T. Aoki, and H. Endo, J. Non-Cryst. Solids **205-207**, 274 (1996).

[20] B.S. Dladla, W.-C. Pilgrim, and F. Hensel, Z. Phys. Chem. (Munich) **199**, 295 (1997).

[21] H. Kohno and M. Yao, J. Phys.: Condens. Matter **13**, 10 293 (2001).

[22] M. Levin and R.W. Schmutzler, J. Non-Cryst. Solids **61&62**, 83 (1984).

[23] F. Hensel, Adv. Phys. **44**, 3 (1995).

[24] M.A.C. Devillers and R.G. Ross, J. Phys. F: Met. Phys. **5**, 73 (1975).

[25] H. Overhof, H. Uchtmann, and F. Hensel, J. Phys. F: Met. Phys. **6**, 523 (1976).

[26] P. Fritzson and K.-F. Berggren, Solid State Commun. **19**, 385 (1976).

[27] L.F. Mattheiss and W.W. Warren, Jr., Phys. Rev. B **16**, 624 (1977).

[28] R.N. Bhatt and T.M. Rice, Phys. Rev. B **20**, 466 (1979).

[29] J.R. Franz, Phys. Rev. Lett. **57**, 889 (1986).

[30] L.A. Turkevich and M.H. Cohen, Phys. Rev. Lett. **53**, 2323 (1984).

[31] W. Hefner and F. Hensel, Phys. Rev. Lett. **48**, 1026 (1982).

[32] R. Winter, T. Bodensteiner, W. Gläser and F. Hensel, Ber. Bunsenges. Phys. Chem. **91**, 1327 (1987); G. Franz, W. Freyland, W. Gläser, F. Hensel, and E. Schneider, J. Phys. (Paris) Colloq. **41**, C8-194 (1980); R. Winter, C. Pilgrim, F. Hensel, C. Morkel, and W. Gläser, J. Non-Cryst. Solids **156-158**, 9 (1993).

[33] S. Hosokawa, T. Matsuoka, and K. Tamura, J. Phys.: Condens. Matter **3**, 4443 (1991).

[34] K. Tamura and S. Hosokawa, J. Phys. (Paris), Colloq. **1**, 39 (1991).

[35] K. Tamura and S. Hosokawa, Phys. Rev. B **58**, 9030 (1998).

[36] G. Kresse and J. Hafner, Phys. Rev. B **55**, 7539 (1997).

[37] S. Munejiri, F. Shimojo, and K. Hoshino, J. Phys.: Condens. Matter **10**, 4963 (1998).

[38] K. Tamura, M. Inui, I. Nakaso, Y. Oh'ishi, K. Funakoshi, and W. Utsumi, J. Phys.: Condens. Matter **10**, 11 405 (1998).

[39] M. Inui, K. Tamura, Y. Oh'ishi, I. Nakaso, F. Funakoshi, and W. Utsumi, J. Non-Cryst. Solids **250-252**, 519 (1999).

[40] K. Tamura, M. Inui, K. Funakoshi, and W. Utsumi, Nucl. Instrum. Methods Phys. Res. A **467-468**, 1065 (2001).

[41] K. Tamura and M. Inui, J. Phys.: Condens. Matter **13**, R337 (2001).

[42] K. Tamura, M. Inui, and S. Hosokawa, Rev. Sci. Instrum. **70**, 144 (1999).

[43] S. Sasaki, KEK Report No. 90-16 (1990).

[44] *International Tables for X-ray Crystallography*, edited by Kathleen Lonsdale (Kynoch Press, Birmingham, 1974), Vol. IV, Table 2.2B.

[45] D.T. Cromer and J.B. Mann, J. Chem. Phys. **47**, 1892 (1967).

[46] X. Hong, M. Inui, T. Matsusaka, D. Ishikawa, M.H. Kazi, and K. Tamura, J. Non-Cryst. Solids **312-314**, 284 (2002).

[47] K. Tamura, M. Inui, T. Matsusaka, D. Ishikawa, M.H. Kazi, X. Hong, M. Isshiki, and Y. Oh'ishi, J. Non-Cryst. Solids **312-314**, 269 (2002).

[48] R. Kaplow, S.L. Strong, and B.L. Averbach, Phys. Rev. **138**, A1336 (1965).

[49] L. Bosio, R. Cortes, and C. Segaud, J. Chem. Phys. **71**, 3595 (1979).

[50] J.G. Winans and M.P. Heitz, Z. Phys. **133**, 291 (1952); **135**, 406 (1953).

[51] J. Donohue, *Structure of the Elements* (Wiley, New York, 1974), p. 231.

[52] V.M. Nield and P.T. Verronen, J. Phys.: Condens. Matter **10**, 8147 (1998).

[53] T. Arai and R.L. McGreevy, J. Phys.: Condens. Matter **10**, 9221 (1998).

[54] F. Barocchi, F. Hensel, and M. Sampoli, Chem. Phys. Lett. **232**, 445 (1995).

[55] M.H. Cohen and J. Jortner, Phys. Rev. A **10**, 978 (1974).

[56] W.W. Warren, Jr. and F. Hensel, Phys. Rev. B **26**, 5980 (1982).